Archaeological Prospection
Archaeol. Prospect. **18**, 105–115 (2011)
Published online 12 May 2011 in Wiley Online Library
(wileyonlinelibrary.com) DOI: 10.1002/arp.411

Geophysical Signatures of a Roman and Early Medieval Necropolis

Y. QUESNEL[1]*, A. JRAD[1,2], F. MOCCI[3], J. GATTACCECA[1], P.-E. MATHÉ[1], J.-C. PARISOT[1], D. HERMITTE[1], V. DUMAS[3], P. DUSSOUILLEZ[1], K. WALSH[4], C. MIRAMONT[5], S. BONNET[6] AND M. UEHARA[1]

[1] *CEREGE, Aix-Marseille University, CNRS, Aix-en-Provence, France*
[2] *Tunis El-Manar University, Tunisia*
[3] *Centre Camille Jullian, CNRS, MMSH, Aix-en-Provence*
[4] *Department of Archaeology, University of York, UK*
[5] *IMEP, Aix-Marseille University, CNRS, Aix-en-Provence, France*
[6] *Mission Archéologique, Aix-en-Provence, France*

ABSTRACT The Roman and early medieval Richeaume XIII necropolis in Provence (France) was systematically studied using magnetic prospection and electrical resistivity tomography (ERT). Remains of a limestone-made building are embedded in a reddish clay formation bearing iron oxides. This produces an interesting negative magnetic anomaly, whereas the wall itself is resistive. Other dipolar magnetic anomalies are correlated with the location of sepulchres, either covered by roman, strongly magnetized tegulae, or corresponding to burnt layers of cremations. After normal data processing, filtering and modelling are applied to the magnetic field data in order to more precisely define the sources. Constraints using ERT soundings, magnetic property measurements, archaeological and geological data help to build such a source model. This study particularly emphasizes that magnetic prospection combined with ERT profiles should be suitable and sufficient on other necropolis sites in the same geological environment. Copyright © 2011 John Wiley & Sons, Ltd.

Key words: Magnetics; archaeology; electrical resistivity tomography; processing; modelling; necropolis

Introduction

Geophysical methods have been used on archaeological sites for about 70 years because they are non-destructive, fast and easy to perform, even over wide areas (Scollar *et al.*, 1990). Mapping techniques such as magnetics facilitate the targeting of excavations, while vertical imaging of sources is possible with electrical resistivity tomography (ERT) soundings. Alternatively, ground-penetrating radar (GPR) allows three-dimensional reconstructions of archaeological sources, although this method is not used in this study. Some drawbacks include the sensitivity of magnetics to intrusive, recent iron objects, and the influence of water content on ERT cross-sections. Further processing and modelling can be applied on magnetic data to estimate source properties. Constraints given by ERT studies may reduce the non-uniqueness of such modelling (Blakely, 1995; Scollar *et al.*, 1990).

Here we present results of a combined study on a roman and early medieval necropolis located in Provence (France). After a brief introduction of the archaeological context, we describe our systematic data acquisition on this site and analyse magnetic maps and ERT cross-sections. Then magnetic-field-data processing and modelling results are applied and discussed.

The Richeaume XIII necropolis and its morphological context

Archaeological context

The Richeaume XIII necropolis (Figure 1) is located at Domaine Richeaume near Aix-en-Provence

* Correspondence to: Y. Quesnel, CEREGE, University Aix-Marseille III, CNRS, Europôle de l'Arbois, BP80, 13545 Aix-en-Provence cedex 04, France. E-mail: quesnel@cerege.fr

Received 12 October 2010
Accepted 4 April 2011

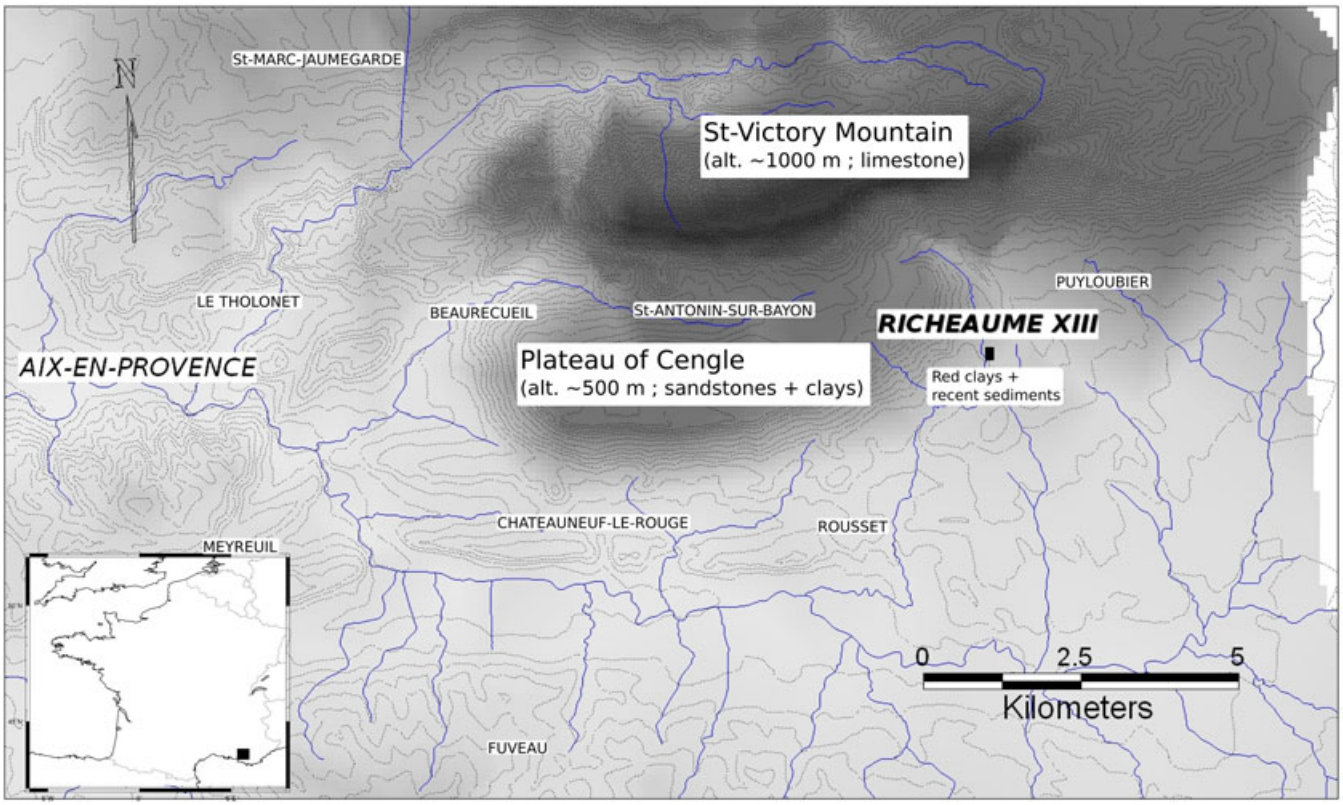

Figure 1. Location of the Richeaume XIII necropolis near Aix-en-Provence. This figure is available in colour online at wileyonlinelibrary.com/journal/arp

(Bouches-du-Rhône, France). The Domaine Richeaume can trace its direct architectural antecedents back to the Roman 'villa' upon which it is situated (Richeaume I; Walsh and Mocci, 2003). In 2004, a complete late Roman inhumation was discovered in the eastern part of the Domaine (Mocci *et al.*, 2008). Following this, a magnetic survey was carried out over a large area on this site. A square-shaped anomaly was detected just north-northeast of the burial (see later). Between 2007 and 2010, archaeological excavations and multidisciplinary research were undertaken (Mocci *et al.*, 2009). The square-shaped magnetic anomaly corresponds to a well-preserved limestone wall of a 166 m^2 room (Figure 2a). Other sepulchres were also discovered on the site: Gallo-Roman cremations and late Roman to early medieval sepulchres covered by tegulae (Figure 2b and c). This suggests that the necropolis was used between the first[t] and the ninth centuries AD, whereas the nearby Roman villa was occupied between the first and sixth centuries AD (Mocci *et al.*, 2005).

Geomorphological context

Located on the left bank of the Naisse stream (altitude 316.55 m), the upper terrace, upon which part of the Richeaume XIII necropolis is situated, consists of coarse alluvial deposits (altitude 326.60–325.05 m). The Naisse stream would have taken a different orientation 2000 years ago, perhaps not as incut as it is today, with the possibility of some flooding on the western side abutting the villa (Walsh and Mocci, 2003; Mocci *et al.*, 2009). These Late Pleistocene terrace deposits are well structured within obliquely intersecting beds, representing torrential alluvial deposits within a braided channel (Jorda and Provansal, 1992; Jorda and Miramont, 2006). The terrace is capped by reworked colluvial units that have been successively ploughed. The archaeological features are within this geological substrate, at depths between 0.20 and 0.60 m. Only the youngest cremations (second century AD Inc5, Inc9 and Inc13 on Figure 3) were situated within thick alluvium that fills the minor depressions around the site.

On top of the limestone substrate, these Late Pleistocene alluvial beds were disturbed by human activity on the site between the last quarter of the first century AD and the first quarter of the second century AD (altitude 325.70–326.45 m). During the third century AD, erosion has disturbed these alluvial units near the eastern and northeast zones of the site, around the

DOI: 10.1002/arp

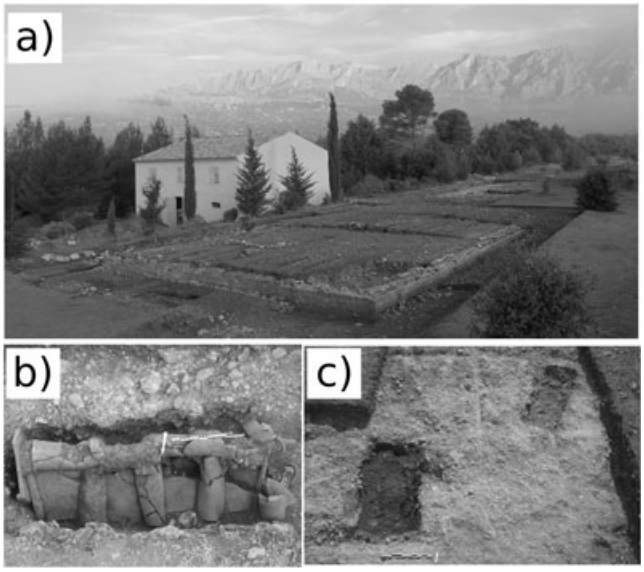

Figure 2. (a) Picture of the Richeaume XIII necropolis (towards NNW), showing the remains of the main building in front. (b) Picture of a Late Roman sepulchre covered by tegulae. (c) Picture of burnt layers resulting from Roman cremation, second century AD. (From L. Damelet, B. Perez and Fl. Mocci, Centre Camille Jullian, Aix-Marseille University-CNRS.)

main building. Minor colluvium of the post-Roman period has mixed with the destruction levels associated with the funerary main building. The last phase of site levelling occurred between the first half of the twentieth century and the 1990s; a period when agricultural activity occurred on the sand and gravel terrace.

Data acquisition and preliminary processing

Magnetics

Instruments and Configuration

Between 2007 and 2009 about 350 m^2 of the site (Figure 3) was studied using magnetic prospection. Two caesium vapour Geometrics G858 magnetometers in vertical gradient configuration were used. Most of the surveys were carried out using predefined rectangles with corners located on the Lambert III projection coordinate of the French mapping system (in metres). Transects were systematically 0.5 m apart with either N–S or E–W orientations. A high sampling rate of 0.1 or 0.3 s was undertaken. The usual heights of the two probes were 0.4 and 0.9 m from the surface, which allows the collection of signals from both shallow (00.5 m) and deep (0.5 3 m) magnetic sources. Prospection at Richeaume XIII was difficult because many small trees and some larger ones prevented us from walking in perfectly straight lines. Therefore, local spatial discrepancies of up to 1 m are possible.

Magnetic Perturbations

Extraneous magnetic signals were produced by many magnetized iron fragments (i.e. millimetre to metre fragments of iron wires) derived from recent agricultural activities and localized either on the ground or within the first 30–40 cm of the soil, although sometimes deeper. We systematically cleaned the area concerned after detection of such pieces using a metal detector and a magnetic gradiometer (Magnetic Locator of Schoensted Ltd.). However, because the three-dimensional location of these objects is not homogeneous and hence may correspond to depths of archaeological materials, we did not remove all unwanted fragments. Therefore many small-wavelength high-amplitude magnetic anomalies may still correspond to such modern objects.

Three datasets were obtained: the magnetic field intensity at 0.4 and 0.9 m height and the vertical magnetic gradient at about 0.65 m. The mean magnetic field intensity at Richeaume XIII between 2007 and 2009 was about 46200 nT. Removal of the external and internal magnetic field is necessary to recover the magnetic anomaly at 0.4 and 0.9 m. No magnetic base station was used. As the usual duration of a survey was 30 min, we checked that surrounding magnetic observatories (CLF in France, EBR in Spain, and AQU in Italy) did not detect strong regional magnetic storms at the time of our surveys. Usually the diurnal variation was less than 2 nT in 30 min, but we corrected the corresponding datasets. The mean magnetic field of the measurements in every line was then subtracted to recover the magnetic anomaly along each line. After these corrections, a nearest-neighbour interpolation using the Generic Mapping Tools (GMT) software (Wessel and Smith, 1991, 1998) was systematically applied to improve the map's coherency. In some cases, magnetic level differences between adjacent lines are still visible, but remain negligible. The geological magnetic level can change across survey areas, but this does not prevent the clear identification of 'archaeological' magnetic anomalies on the maps.

Other Magnetic Measurements

In order to tie the magnetic anomalies with potential magnetized sources on the site, surface magnetic susceptibility measurements were taken on several materials from Richeaume XIII (soil, wall, etc.). A ZH SM30 magnetic susceptibility meter was used for these *in situ* measurements. Table 1 summarizes the magnetic susceptibility data at Richeaume XIII. As

DOI: 10.1002/arp

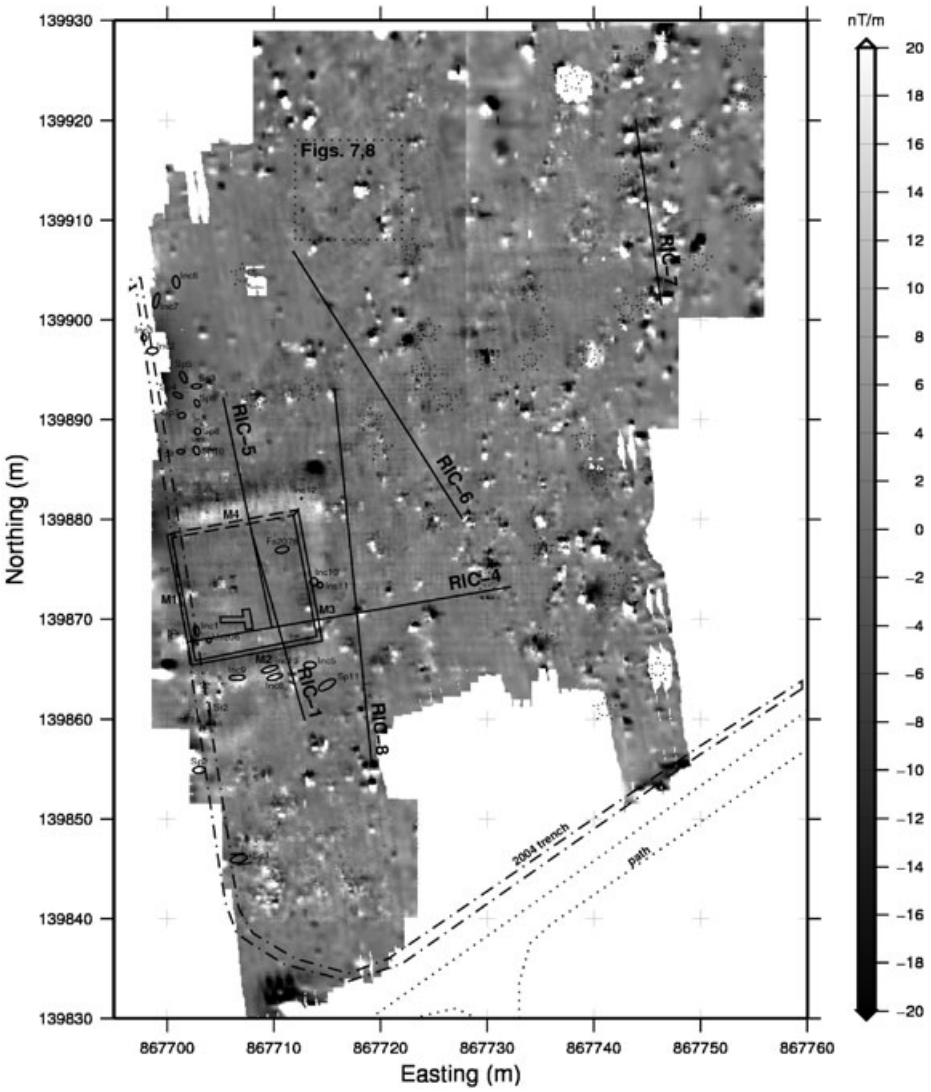

Figure 3. Vertical 0.65-m-high magnetic gradient map over Richeaume XIII. Several datasets of all different surveys are interpolated. Black segments with RIC-x correspond to locations of the ERT soundings. Trees are symbolized by dashed stars. Foreground indicates the archaeological findings and the current Richeaume XIII site. A dashed square in the north shows the selected area for Figures 7 and 8. This map shows the square-shaped anomaly due to a limestone wall embedded in magnetic clays. Other elongated anomalies may correspond to sepulchres covered by tegulae as well as to burnt layers of cremation.

expected, the presence of limestone rock tends to decrease the magnetic susceptibility. The soil at Richeaume XIII is mainly composed of a red clay enriched in iron oxides, leading to a significant magnetic susceptibility of about 0.5×10^{-3} SI. The highest magnetic susceptibility values correspond to burnt materials: Roman tegulae (fired clays) covering some sepulchres and burnt soil layers associated with the cremations. Using a 775R 2G enterprises SQUID magnetometer, we also measured the natural remanent magnetization intensity of some samples of tegulae: the mean value is $1.2 \pm 0.1\,\mathrm{A\,m^{-1}}$, showing that they also possess a significant component of remanent magnetization, like particles of burnt soil (Le Borgne, 1960; Scollar *et al.*, 1990; Jordanova *et al.*, 2001; Linford and Canti, 2001; Kovacheva *et al.*, 2004). Thus, significant magnetic contrasts should produce clear magnetic anomalies at Richeaume XIII.

Electrical resistivity tomography

A total of eight electrical resistivity tomography (ERT) soundings were performed at Richeaume XIII (Figure 3). The instrument was an ABEM Terrameter LUND Imaging System (SAS4000 + ES1064). It was used in a Schlumberger–Wenner reciprocal layout protocol, using a 64 or 128 multi-electrode array with 30 or 50 cm of electrode spacing (see Ritz *et al.* (1999)

DOI: 10.1002/arp

Table 1. Geophysical properties of the materials at Richeaume XIII

Material		Magnetic susceptibility (10^{-3} SI)	Electrical resistivity (Ω·m)
Geological	'Glacis' of limestone pebbles	0.01	>100
	Red clays	0.50	<100
Archaeological	Wall in limestone	0.01	>500
	Sepulchres with *tegulae*	2.00	>300
	Burnt layers (cremations)	2.00	100–300

for a complete description of the method). The profile lengths were 19 m (RIC-1 and –7), 31.5 m (RIC-4 and –6) or 38 m (RIC-8), corresponding to about 2.5, 4 and 6 m of investigated soil thicknesses, respectively. After acquisition (about 1 h), the RES2DINV software (GEOTOMO SOFTWARE Sdn. Bhd.) was used to derive a reasonable model for the distribution of the true electrical resistivity along each profile. In this study, only resulting ERT cross-sections of RIC-1 (see Figure 5) and RIC-7 (see Figure 6) are presented and discussed later, because they show interesting conductive/resistive anomalies of the ground of this site.

The mean electrical resistivity values of the materials at Richeaume XIII that were derived from these soundings as well as from excavations are shown in Table 1. The most resistive material is the limestone, essentially composing the wall of the main building, whereas the red clay soil is conductive, depending on the water content. Sepulchres can be either highly resistive or significantly conductive, depending on the filling material. Then, the identification of both magnetic anomalies and electrical resistivity anomalies should clearly help to constrain the buried sources.

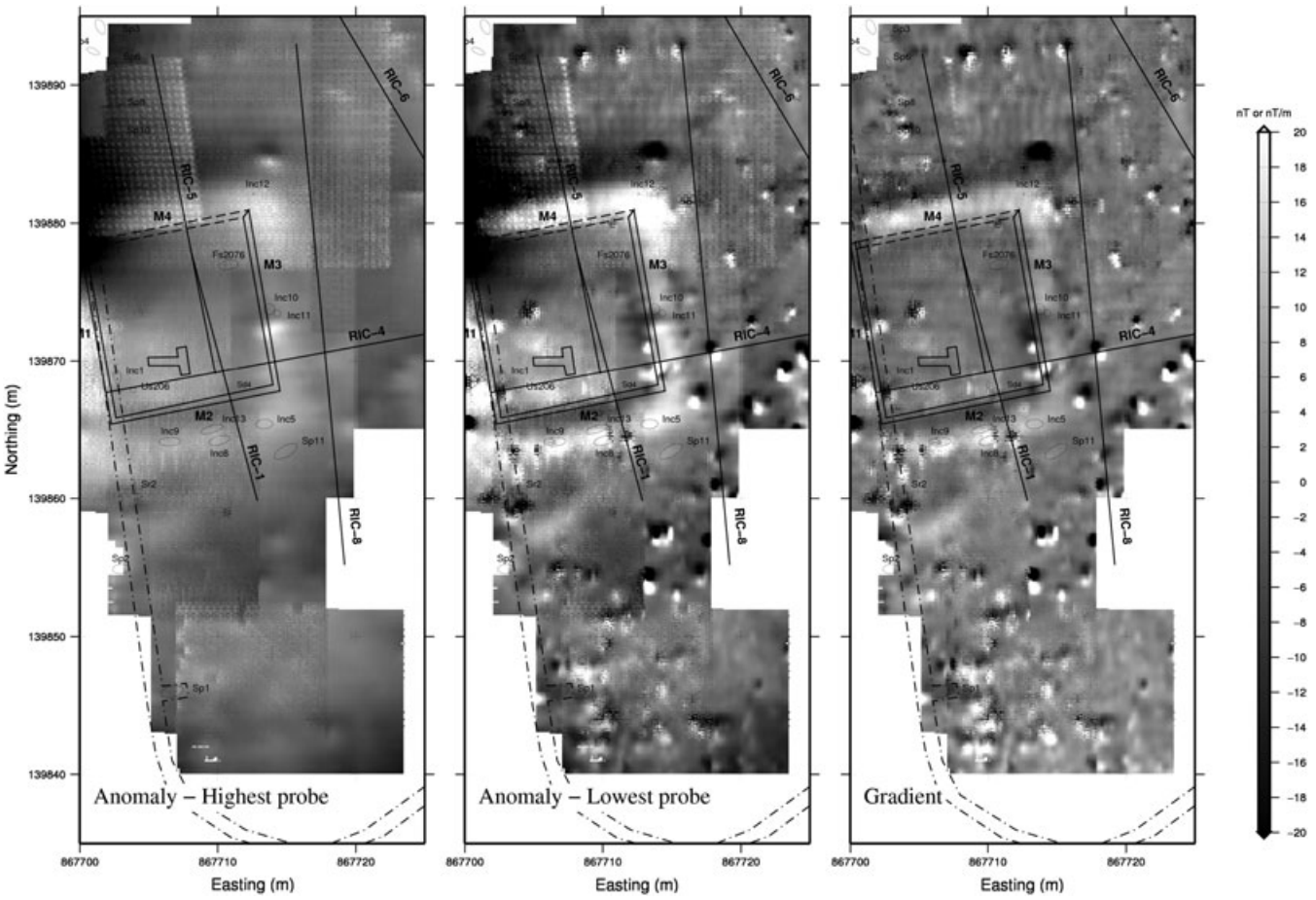

Figure 4. Interpolation of the magnetic surveys over the building. Walls of the building are M1 to M4, the latter shown as dashed lines as they have so far not been excavate.

DOI: 10.1002/arp

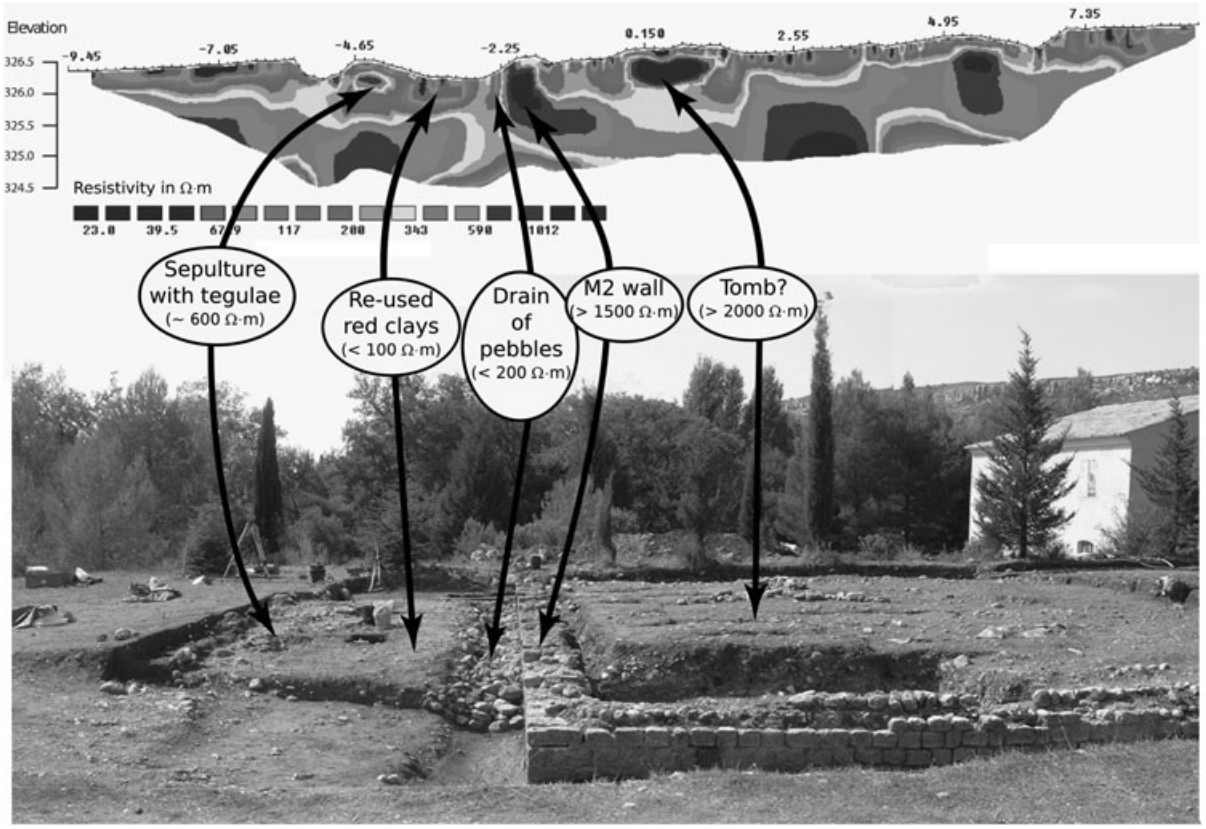

Figure 5. Electrical resistivity derived from the RIC-1 ERT sounding and correspondence with the Richeaume XIII materials.

Results

In this section we detail the resulting magnetic maps and ERT cross-sections used to identify potential archaeological features.

Magnetic maps

Figure 3 shows a global magnetic view of the site. The most important feature of this map is the square-shape high gradient on the western side of the area, corresponding to remains of the limestone walls of a 166 m^2 building (Figure 2). After excavation, we discovered that the negative part of the linear magnetic anomalies and gradient (Figure 4) could be associated with the non-magnetic limestone wall on the south, but not on the north. Indeed, the Roman builders reused red clays from the surrounding soil: this magnetic formation was situated on the exterior of each wall, and these are thickened and strengthened by a narrow drain of limestone pebbles. This then produces a dipolar east–west elongated magnetic anomaly and gradient just adjacent to both the north (M4) and south (M2) walls.

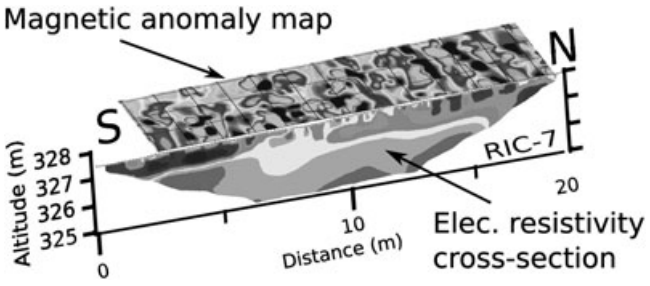

Figure 6. Perspective view showing the correlation between electrical resistivity derived from the RIC-7 ERT sounding and the magnetic anomalies over this profile.

DOI: 10.1002/arp

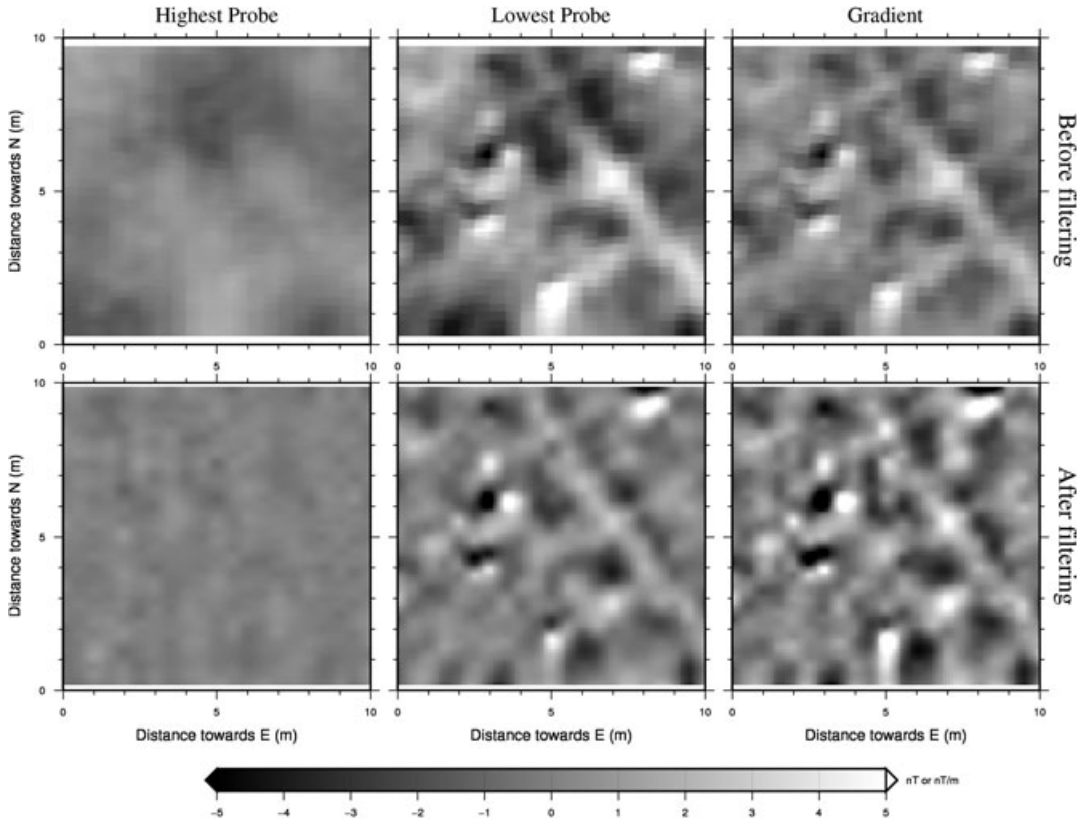

Figure 7. Comparison between observed and filtered data in a section centred on ($X = 867717$ m, $Y = 139913$ m) indicated by the dashed square on Figure 3.

Excavations also reveal, at least on the southern and northern sides of the building, that these reused clays contain sepulchres (Sp-x) and cremations (Inc-x), which tend to enhance the positive magnetic signal. Some of the burnt units comprise a 1 to 3 cm thick burnt layer, whereas others contain few burnt particles. Hence there is no typical magnetic signal over these cremations. Only those located to the south and near the building (Inc9, Inc3 and Inc8) are very magnetic and thus influence the observations. Similarly, all sepulchres are not covered by magnetic tegulae, which results in different magnetic field intensity due to such structures. As some sepulchres seem to be approximately 1–2 m long in an east–west direction, then it is possible to identify some of these by association with elongated magnetic field anomalies, such as those located near (139918 m N, 867745 m E) and near (139855 m N, 867719 m E) on the global map (Figure 3). No excavations have been undertaken here until now. All other magnetic anomalies and areas of high gradients (outside of excavation zones) are difficult to associate with any potential archaeological structures or objects. Indeed the small-wavelength high-amplitude signal of recent iron objects is probably at the origin of most of these anomalies.

Electrical resistivity tomography cross-sections

Figure 5 illustrates the correlation between electrical resistivity anomalies and excavation along a north–south profile (RIC-1 on Figure 3) that crosses the south wall of the building. As expected, the limestone wall clearly appears with high resistivity up to 2000 Ω·m. This suggests that another negative magnetic anomaly on the site, associated with a large positive resistivity anomaly, may correspond to another limestone structure. In this sounding, the sepulchre appears resistive (about 500–700 Ω·m), but less than the wall; isolated dipolar magnetic anomalies plus relatively high resistivities should indicate the presence of sepulchres in the soil. By way of contrast, reused clays are very conductive but create wide dipolar magnetic anomalies, while the narrow drain of limestone pebbles is more resistive, but should enhance the negative magnetic signal of the wall itself. Thus combining these two geophysical parameters (electrical resistivity and magnetics) should constrain

DOI: 10.1002/arp

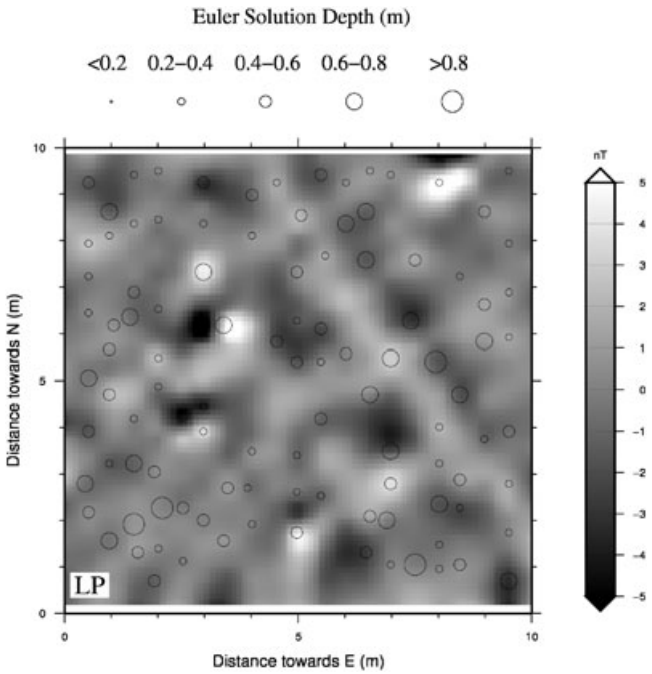

Figure 8. Example of source-depth determination using Euler deconvolution with structural index of 2. Same area as for Figure 7, lowest probe.

our determination of other buried potential archaeological sources on the site. For instance, this RIC-1 profile on Figure 5 indicates that a wide and very resistive anomaly is present inside the building. The magnetic field anomaly at this location is weak (Figure 4) but not negative. Probably the presence of red clays in the soil inside the building may tend to increase the magnetic field. Then our interpretation for this source (still not excavated) is a block of limestone that may correspond to a tomb marking an important sepulchre or to a 'natural' altar. The RIC-7 sounding shows many resistive but shallow anomalies. Interestingly, they correlate very well with some east–west elongated magnetic anomalies (Figure 6). Either wide and deep ploughing tracks or sepulchres could generate such signal.

Discussion

Integration of magnetic data, ERT soundings and excavations clearly helped to understand the Richeaume XIII necropolis. However, our magnetic vision of the site is still disturbed by signals produced by modern iron debris. Indeed numerous small dipolar anomalies are observed on the map (Figure 3). At their worst, some of these modern objects can create 1- or 2-m-long anomalies: then the distinction between anomalies due to sepulchres or cremations and anomalies due to this debris becomes very difficult. One needs to apply further processing to eventually remove unwanted signals. Another approach is to model the potential archaeological sources in order to simulate their true signals and to compare these with our observations. Attempts to perform these two approaches are detailed in the next two sections.

Further processing

Different types of bandpass filters were first applied using a portion of the dataset where some anomalies may correspond to true archaeological sources (Figure 7, top panels), whereas others may correspond to recent shallow iron objects. Standard Butterworth bandpass filter cutting wavelengths smaller than 0.3 m and greater than 4 m reveals a NW–SE linear feature (a ditch?) previously observed on the raw anomaly map (lowest probe). The filtering reveals that this structure crosses all the eastern part of the area selected (Figure 7, bottom panels). Other linear features (recent ploughing traces?) perpendicularly crossing the previous anomaly were seen on the raw gradient map, but the filter does not seem to amplify them. Therefore such filtering processes should be used with care.

Other isolated dipolar magnetic anomalies are observed in the same selected area in ($X = 2.5$ m, $Y = 4$ m) and in ($X = 3$ m, $Y = 6$ m). Several pieces of iron were found at these places. However, the filtering, instead of erasing these signals, seems to highlight their true 1-m-long and dipolar shape. Thus we can conclude that such a technique is suitable to clarify the magnetic anomaly map, but not to erase anomalies due to magnetic debris. Indeed these recent iron objects are either a high concentration of very small pieces of barbed wires, or isolated bent iron wire. Thus the resulting magnetic anomaly signal is very intense and often as wide as an anomaly caused by a cremation ditch.

Further modelling

To separate anomalies caused by recent debris from those due to archaeological sources, one can also use a 'depth threshold' using the ANalytical signal and EULer deconvolution (ANEUL) method (Reid *et al.*, 1990; Salem and Ravat, 2003). Here Geosoft Oasis montaj software was used on the same selected area as in the previous section. Shallow (0–40 cm) anomaly sources probably corresponding to iron debris were thus detected including at ($X = 2.5$ m, $Y = 4$ m) on the

DOI: 10.1002/arp

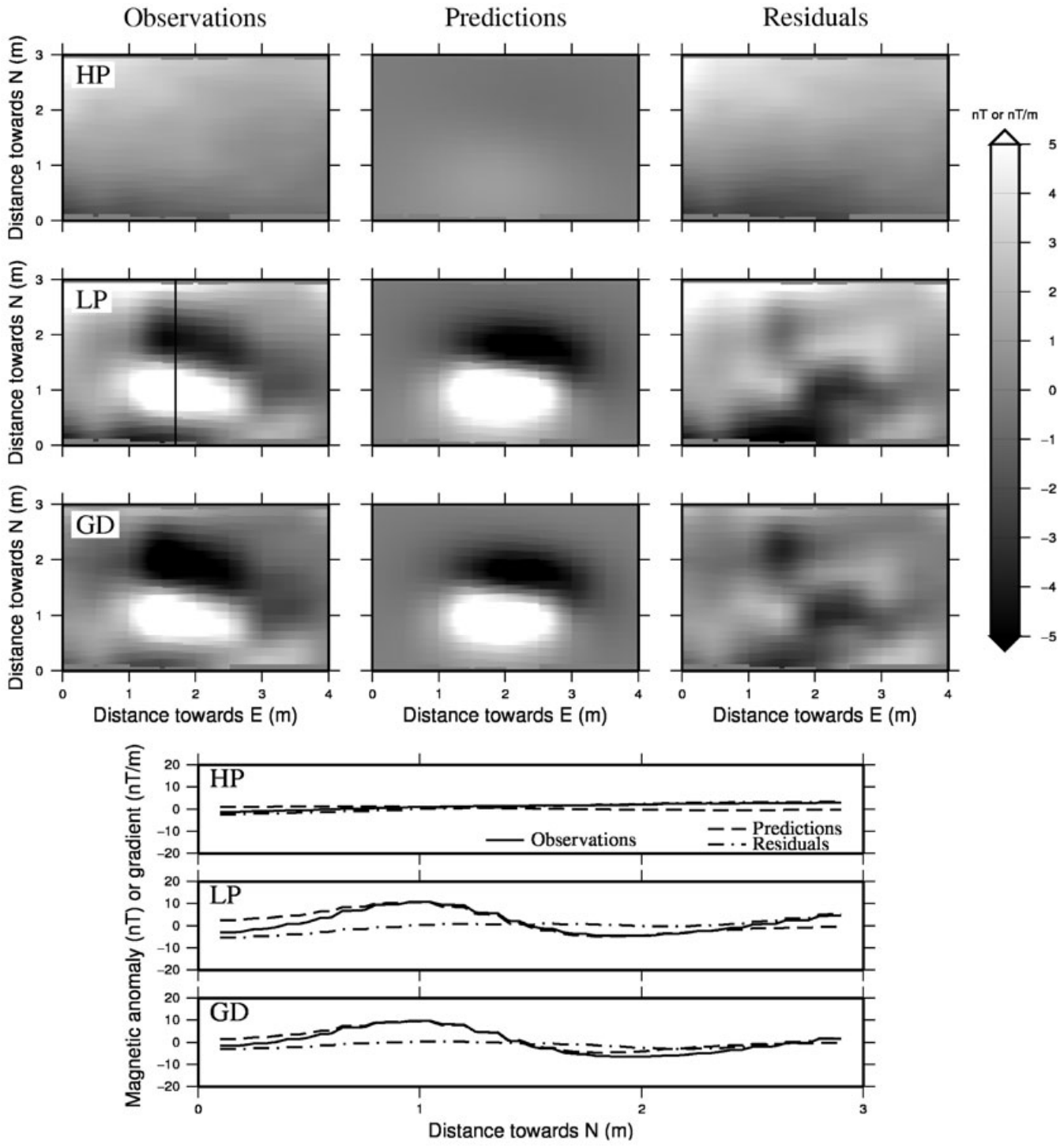

Figure 9. (Top panels) Comparison between observed and predicted data in a section of the studied area, over a sepulchre covered by tegulae: HP, LP and GD mean highest probe, lowest probe and gradient maps, respectively. Predictions were calculated using a uniformly magnetized rectangular prism with parameters of Table 2. (Bottom panels) Same comparison using the profile crossing the anomaly, and shown by a black line on the LP observation image of the top panels.

Euler source resulting map (Figure 8). Its northern neighbour at ($X = $ m, $Y = 6$ m) is deeper and so may correspond to a true archaeological source. Another way to improve our source determination is to model potential sources (recent or archaeological ones), simulate their signal and compare it with the

DOI: 10.1002/arp

Table 2. Parameters of the best uniformly magnetized rectangular prism modelling a sepulchre

NS/EW Extension (m)	Top (m)	Bottom (m)	Magnetization intensity ($A\,m^{-1}$)	Magnetic inclination (°)	Magnetic declination (°)
0.75/1.40	0.3	0.6	0.15	30.0	30.0

observations. Here we try to model a sepulchre or a cremation layer using a uniformly magnetized rectangular prism. The initial magnetization parameters for the prism and the surroundings are constrained by our *in situ* susceptibility measurements, whereas its extent and thickness are constrained by ERT results and excavations. Best parameters are found by forward modelling, specifying as input reasonable ranges for each parameter, although inversion using least-square criterion is also possible. The complete method is detailed in Quesnel *et al.* (2008).

The observations shown in Figure 9 (left column in top panels) were acquired on one of the sepulchres. Its tegulae roofing measures 120 cm east–west with a width of 40 cm. The best fit between observations and predictions correspond to the prism parameters shown in Table 2. The depth correlates very well with the summit and base of the tegulae roofing, and surface extensions are also close to the observed values. This reveals that the magnetization should be partly remanent (i.e. different from the direction of the local main magnetic field) to fit the observations. This magnetization vector may result from the combination of the magnetization vectors of all tegulae with different orientations in this 'roof'. Such simulations should serve to clearly identify other similar sepulchres on this site as well as on other necropolis.

Conclusions

In archaeological prospection it is common to consider how to localize (in three dimensions) structures or objects in the soil with non-destructive techniques and how to characterize them (ceramics?, limestone wall?, etc.). The latter implies going further than producing a simple magnetic map. Here the results from ERT soundings, from magnetic property measurements as well as from filtering and modelling of the magnetic field data were integrated to identify archaeological sources on a Roman and early medieval necropolis in Provence (France). While the magnetic surveys themselves allowed us to localize a wall and some sepulchres or cremations, ERT soundings gave information on their depths. Magnetic susceptibility and electrical resistivity were used to further characterize their materials. Filtering did help to clarify some linear structures on the site, however, it did not erase signals of recent and shallow iron debris, whereas the Euler deconvolution allowed us to exclude them. Finally, localized forward modelling using a prism seems to be appropriate to represent a sepulchre covered by tegulae.

Acknowledgements

The authors would like to thank the French Culture Ministery DRAC - SRA PACA. All students and archaeologists involved in the cited field campaigns are particularly acknowledged, as well as P. Rochette, F. Demory, G. Granier, T. Bartette, C. Cenzon-Salvayre, N. Coquet, the two reviewers and C. Gaffney. Some figures were produced using the GMT software (Wessel and Smith, 1991, 1998).

References

Blakely R. 1995. *Potential Theory in Gravity and Magnetic Applications*. Cambridge University Press: Cambridge.

Jorda M, Miramont C. 2006. Caractéristiques du milieu naturel du Val de Durance au bassin d'Aix-en-Provence. In *Aix-en-Provence, Pays d'Aix, Val de Durance. Carte Archéologique de la Gaule*, 13/4, Mocci F, Nin N (eds). Académie des Inscriptions et des Belles Lettres: Paris; 121–124.

Jorda M, Provansal M. 1992. La montagne Sainte Victoire, Structure, relief et morphogénèse antérieure au Postglaciaire. *Méditerrannée*, **1**(2): 17–28.

Jordanova N, Petrovsky E, Kovacheva M, Jordanova D. 2001. Factors determining magnetic enhancement of burnt clay from archaeological sites, *Journal of Archaeological Science* **28**: 1137–1148. doi:10.1006/jasc.2000.0645.

Kovacheva M, Hedley I, Jordanova N, Kostadinova M, Gigov V. 2004. Archaeomagnetic dating of archaeological sites from Switzerland and Bulgaria, *Journal of Archaeological Science* **31**: 1463–1479. doi:10.1016/j.jas.2004.03.019.

Le Borgne E. 1960. Influence du feu sur les propriétés magnétiques du sol et sur celles du schiste et du granite. *Annals of Geophysics* **16**(2): 159–199.

Linford N, Canti M. 2001. Geophysical evidence for fires in antiquity: preliminary results from an experimental study (Paper Given at the EGS XXIV General Assembly in The Hague, April 1999. *Archaeological Prospection* **8**: 211–225. doi:10.1002/arp.170.

Mocci F, Walsh K, Dumas V, *et al*. 2005. Aqueducs et structures hydrauliques de la villa antique de Richeaume (Puyloubier, 13). *Gallia* **62**: 147–160.

Mocc F, Perez B, Dumas V. 2008. Les sépultures du site de Richeaume XIII: premiers témoignages d'une nécropole domaniale sur le piémont méridional de la Sainte-Victoire (Puyloubier, 13)? In *Archéologie de Provence et d'ailleurs (Mélanges offerts à G. Congès et G. Sauzade)*, Vol. **5**, Brochier J-E, Guilcher A, Pagni M (eds). Supplément Bulletin Archéologique de Provence Aix-en-Provence, pp. 505–518.

Mocci F, Granier G, Dumas V, *et al*. 2009. *Rapport final d'opération sur le site de Richeaume XIII (Puyloubier, 13), Opération archéologique programmée triannuelle 2007–2009*, **2** Vols. Centre Camille Jullian – French Ministery of Culture: Aix-en-Provence; 435 pp.

Quesnel Y, Langlais B, Sotin C, Galdéano A. 2008. Modeling and inversion of local magnetic anomalies. *Journal of Geophysics and Engineering* **5**: 387–400. doi:10.1088/1742-2132/5/4/003.

Reid A, Allsop J, Granser H, Millett A, Somerton I. 1990. Magnetic interpretation in three dimensions using Euler deconvolution, *Geophysics* **55**(1): 80–91.

Ritz M, Parisot J, Diouf S, Beauvais A, Dione F, Niang M. 1999. Electrical imaging of lateritic weathering mantles over granitic and metamorphic basement of eastern Senegal, West Africa. *Journal of Applied Geophysics* **41**(4): 335–344.

Salem A, Ravat D. 2003. A combined analytic signal and Euler method (AN-EUL) for automatic interpretation of magnetic data. *Geophysics* **68**(6): 1952–1961.

Scollar I, Tabbagh A, Hesse A, Herzog I. 1990. *Archaeological Prospecting and Remote Sensing*. Cambridge University Press: Cambridge.

Walsh K, Mocci F. 2003. Fame and marginality: The archaeology of Montagne Sainte Victoire (Provence, France). *American Journal of Archaeology* **107**: 45–70.

Wessel P, Smith WHF. 1991. Free software helps map and display data. *EOS Transactions* **72**: 441–441. doi:10.1029/90EO00319.

Wessel P, Smith WHF. 1998. New, improved version of generic mapping tools released. *EOS Transactions* **79**: 579–579. doi:10.1029/98EO00426.

DOI: 10.1002/arp